

Ferromagnetic coupling of $[\text{Ni}(\text{dmit})_2]^-$ anions in $(m\text{-fluoroanilinium})(\text{dicyclohexano}[18]\text{crown-6})[\text{Ni}(\text{dmit})_2]^\ddagger$

Tomoyuki Akutagawa,^{*a,b} Daisuke Sato,^b Qiong Ye,^a Shin-ichiro Noro^{a,b} and Takayoshi Nakamura^{*a,b}

Received 2nd October 2009, Accepted 14th December 2009

First published as an Advance Article on the web 15th January 2010

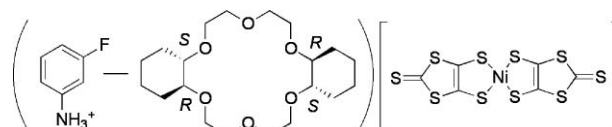
DOI: 10.1039/b920600k

Ferromagnetic coupling of the $[\text{Ni}(\text{dmit})_2]^-$ anion layer through lateral sulfur–sulfur interactions along the short-axis of the anion was achieved using the flexible supramolecular cation of $(m\text{-fluoroanilinium}^+)(\text{meso-dicyclohexano}[18]\text{crown-6})$.

Ferromagnetic ordering of metal–organic coordination compounds has been reported in $[\text{Fe}(\text{C}_5\text{Me}_5)_2][\text{tetracyanoethylene}]$, $\text{MnCu}[2\text{-hydroxy-1,3-propylenebis(oxamato)}]\cdot\text{H}_2\text{O}$, and $[\text{Ni}(1,1\text{-dimethylethylenediamine})_2][\text{Fe}(\text{CN})_6]\text{CF}_3\text{SO}_3\cdot 3.5\text{H}_2\text{O}$,¹ where the magnetic exchange energy (J) between the metal centers plays an important role in achieving a positive J value. The π -orbitals of the organic ligands consist of the frontier orbitals of several metal–organic compounds such as $[\text{Ni}(\text{mnt})_2]^-$ and $[\text{Ni}(\text{dmit})_2]^-$ anions, where mnt^{2-} and dmit^{2-} are maleonitriledithiolate and 2-thioxo-1,3-dithiole-4,5-dithiolate, respectively.² The effective contribution of the Ni orbital to the LUMO orbital of the $[\text{Ni}(\text{mnt})_2]^-$ anion results in ferromagnetic ordering of $\text{NH}_4^+[\text{Ni}(\text{mnt})_2]\cdot\text{H}_2\text{O}$ at 4.5 K.³ On the other hand, since the LUMO orbital of the $[\text{Ni}(\text{dmit})_2]^-$ anion was constructed from the π -orbital of dmit^{2-} ligands,² the J value between the $[\text{Ni}(\text{dmit})_2]^-$ anions was smaller than those of the $[\text{Ni}(\text{mnt})_2]^-$ anion. However, the LUMO orbital is delocalized onto the entire $[\text{Ni}(\text{dmit})_2]^-$ anion, and can participate in diverse intermolecular interactions such π -stacking, π -dimers, lateral dimers, and linear-chains. These conformations are thought to be responsible for the diverse magnetic properties observed.⁴

We previously reported a useful technique to control the $[\text{Ni}(\text{dmit})_2]^-$ anion arrangements using supramolecular cation structures of organic ammonium–crown ether assemblies. For example, $(\text{anilinium}^+)([18]\text{crown-6})$, $(p\text{-xylylenediammonium}^+)([18]\text{crown-6})_2$, and $\text{meso-1,2-diphenylethylenediammonium}^+([18]\text{crown-6})_2$ supramolecules yielded the spin-ladder, π -dimer, and two-dimensional square lattice of $S = 1/2$ spin on the $[\text{Ni}(\text{dmit})_2]^-$ anions.⁵ One aspect of this approach is the possible structural diversity in terms of size, valence, and flexibility of the cation structures. In addition, dynamic cation structures such as molecular rotators can be designed in $[\text{Ni}(\text{dmit})_2]^-$ salts,^{4,6}

in which molecular motions can couple with J values. Herein, we report a new $[\text{Ni}(\text{dmit})_2]^-$ salt with ferromagnetic coupling ($J > 0$) induced by the $(m\text{-FAni}^+)(\text{DCH}[18]\text{crown-6})$ supramolecular cation (Scheme 1).



Scheme 1 Molecular structures of $m\text{-fluoroanilinium}$ ($m\text{-FAni}^+$), $\text{meso-dicyclohexano}[18]\text{crown-6}$ ($\text{DCH}[18]\text{crown-6}$), and $[\text{Ni}(\text{dmit})_2]$.

Slow diffusion between $(n\text{-Bu}_4\text{N}^+)[\text{Ni}(\text{dmit})_2]^-$ and $(m\text{-FAni}^+)(\text{BF}_4^-)$ in the presence of $\text{DCH}[18]\text{crown-6}$ yielded single crystals of $(m\text{-FAni}^+)(\text{DCH}[18]\text{crown-6})[\text{Ni}(\text{dmit})_2]^-$ (**1**).[‡] The 1:1 adduct of the supramolecular cation between $m\text{-FAni}^+$ and $\text{DCH}[18]\text{crown-6}$ was observed through the six $\text{N-H}^+ \sim \text{O}$ hydrogen bonds, forming a stand-up configuration of the C-NH_3^+ unit of $m\text{-fluorophenyl}$ groups with respect to the mean oxygen plane of the $\text{DCH}[18]\text{crown-6}$ (Fig. 1a). The average N-O hydrogen-bonding distances between the ammonium nitrogen and six oxygen atoms of $\text{DCH}[18]\text{crown-6}$ ($d_{\text{N-O}} = 2.914 \text{ \AA}$) was comparable to the standard $\text{N-H}^+ \sim \text{O}$ hydrogen bond length.⁷ The fixed orientation of $m\text{-FAni}^+$ suggested restriction of the molecular motions of $m\text{-FAni}^+$ due to the steric hindrance

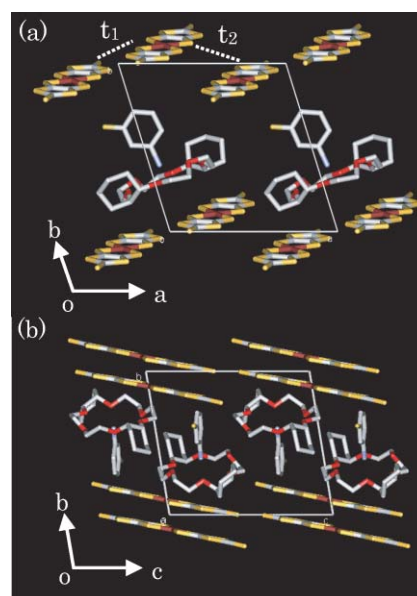


Fig. 1 Crystal structure of salt **1**. Unit cell viewed along (a) the c -axis and (b) the a -axis.

^aResearch Institute for Electronic Science, Hokkaido University, Sapporo, 001-0020, Japan. E-mail: takuta@es.hokudai.ac.jp, tnaka@es.hokudai.ac.jp; Fax: 81-11-7069420; Tel: 81-11-7069418

^bGraduate School of Environmental Earth Science, Hokkaido University, Sapporo, 060-0810, Japan

[‡] Electronic supplementary information (ESI) available: Crystal growth, atomic numbering scheme, structural analysis of salt **1**, calculated model structures, IR spectra, Raman spectra, dielectric measurements, potential energy curve for molecular rotation, and DFT calculation. CCDC reference numbers 749640 & 749641. For ESI and crystallographic data in CIF or other electronic format see DOI: 10.1039/b920600k

from the two nearest-neighboring cyclohexane rings. However, increasing the temperature changed the thermal parameter of the fluorine atom from $B_{\text{eq}} = 2.58$ at 100 K to $B_{\text{eq}} = 8.66$ at 300 K, suggesting that thermal fluctuation of $m\text{-FAni}^+$ occurred around room temperature.

Fig. 1a and 1b show the unit cell of salt **1** viewed along the c - and a -axis, respectively. The cation–anion packing in salt **1** is the same as that of (anilinium⁺)(DCH[18]crown-6)[Ni(dmit)₂][−] (**2**).⁴ Alternating layers of cations and anions were elongated along the b -axis. The transfer integral was based on extended Hückel molecular orbital calculations and was used to evaluate the magnitude of the intermolecular interactions between the [Ni(dmit)₂][−] anions within the crystal.²¹ The two-dimensional [Ni(dmit)₂][−] layer was observed in the ac -plane, where lateral sulfur–sulfur contacts ($t_1 = -1.21$ meV and $t_2 = 2.27$ meV) were observed along the a -axis. Two other interactions of $t_3 = -10.0$ meV and $t_4 = -2.76$ meV connected the lateral dimer along the c -axis. Our previous findings showed that a uniform [Ni(dmit)₂][−] interaction along the long axis of the anion resulted in a one-dimensional antiferromagnetic Heisenberg chain. The same ferromagnetic coupling has been confirmed in the isomorphous salt **2**, where the lateral J_1 - and J_2 -interactions were essential for the ferromagnetic coupling.

Fig. 2b shows the ($m\text{-FAni}^+$)(DCH[18]crown-6) cation arrangement in the ac -plane. The orientation of the $m\text{-FAni}^+$ cation was fixed in the layer. The molecular motion of $m\text{-FAni}^+$ in the solid state was evaluated by the potential energy curve and the magnitude of the potential energy barrier (ΔE), which was calculated using the RHF/6-31(d) basis set with the atomic coordinates determined from the X-ray crystal structural analysis.⁸ The two nearest-neighboring DCH[18]crown-6 were included in

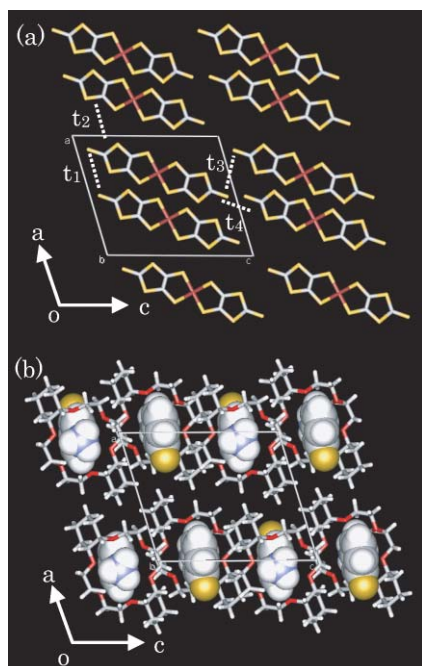


Fig. 2 Cation–anion arrangements in salt **1**. (a) Two-dimensional [Ni(dmit)₂][−] anion arrangement within the ac -plane. The intermolecular J are depicted in the ac -plane. (b) The supramolecular cationic layer in the ac -plane. The $m\text{-FAni}^+$ is shown by van der Waals representations.

the calculations taking the steric repulsions into account (see Fig. S5[†]). An asymmetrical double-minimum type potential energy curve with large ΔE values of 3200 and 1600 kJ mol^{−1} was obtained. Although the same cation–anion arrangements were observed in salt **2** with $\Delta E \sim 330$ kJ mol^{−1}, the modification of the cation structure from An⁺ to $m\text{-FAni}^+$ significantly enhanced ΔE for the flip-flop motion of the cation. Such a dipole inversion was not allowed in salt **1** due to quite a high potential energy barrier.

The temperature- and frequency-dependent dielectric constant (ϵ_1) of salt **1** showed a slight anomaly around 240 K (Fig. 3). The crystal structure and large ΔE values confirmed that the small amplitude thermal fluctuation of $m\text{-FAni}^+$ can affect the dielectric responses. A small hump in the ϵ_1 – T plots was observed along the a -axis, parallel to the π -plane of $m\text{-FAni}^+$. From the potential energy calculations, small amplitude thermal fluctuations within the limit of $\pm 20^\circ$ were assigned to a pendulum motion of the $m\text{-FAni}^+$ cation. Since the dielectric anomaly along the c -axis was not observed, the pendulum motion of $m\text{-FAni}^+$ occurred along the a -axis at temperatures above 240 K. The dielectric response at 1 kHz was larger than that at 1 MHz, therefore, a slow molecular motion around room temperature influenced the dielectric properties of the crystal. The constant ϵ_1 value (~ 275) at temperatures below 150 K was due to the polarization of π -electrons along the short-axis of the [Ni(dmit)₂][−] anion.

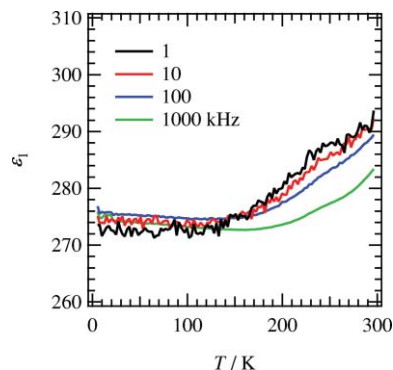


Fig. 3 Temperature- and frequency- (1, 10, 100, and 1000 kHz) dependent dielectric constants (ϵ_1) of salt **1** along the a -axis. The a -direction was parallel to the π -plane of $m\text{-FAni}^+$.

The molar magnetic susceptibility (χ_{mol}) was dominated by the [Ni(dmit)₂][−] anion arrangements in the crystal. The Curie–Weiss behavior with a ferromagnetic coupling (Curie constant $C = 0.375$ emu K mol^{−1} and Weiss temperature $\theta = +3.42$ K) was observed in the $\chi_{\text{mol}}T$ – T plots (Fig. 4a). Increasing the $\chi_{\text{mol}}T$ values with a decrease in temperature below 70 K clearly showed ferromagnetic coupling between [Ni(dmit)₂][−] anions. The magnetization (M)–magnetic field (H) plots at 2 K resulted in an S-shaped response with a saturation of the M value at 1.73 μ_B , which corresponded to one $S = 1/2$ spin. The hysteresis in the M – H curve was not detected at 2 K, and the AC magnetic susceptibility showed no evidence for the ferromagnetic ordering at 2 K (Fig. S6[†]). To evaluate the J_1 – J_4 interactions, symmetry-broken DFT calculations were applied for each pair.^{9,10} The UB3LYP method using the basis-set of Ni atoms for a triple-zeta type designed for an ECP + f polarization (LanL2TZ) and those of S and C atoms for an aug-cc-pVDZ were employed for the calculations. The J value was defined by $(E_{\text{singlet}} - E_{\text{triplet}})/(\langle S^2 \rangle_{\text{singlet}} - \langle S^2 \rangle_{\text{triplet}})$, where E and

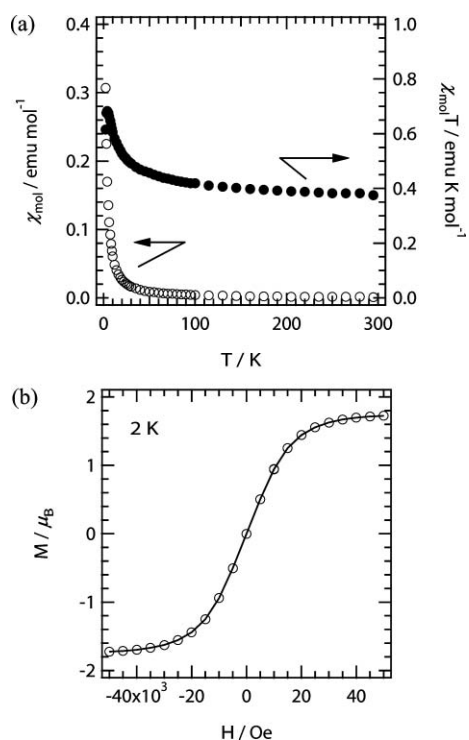


Fig. 4 Magnetic properties of salt 1. (a) χ_{mol} vs. T plots (left-scale) and $\chi_{\text{mol}}T$ vs. T plots (right-scale) and (b) M – H plots at 2 K.

$\langle S^2 \rangle$ are the total energy and the total spin angular momentum, respectively. The magnitude of the J_1 - and J_2 -interactions were significantly smaller than those for the J_3 - and J_4 -interactions (see Table S2†), suggesting that the energy difference between the singlet and triplet states was small for the lateral $[\text{Ni}(\text{dmit})_2]^-$ anion arrangements.

In conclusion, an alternate layer of supramolecular cations and anions was observed in $(m\text{-FAni}^+)(\text{DCH}[18]\text{crown-6})[\text{Ni}(\text{dmit})_2]^-$. The two-fold rotation of $m\text{-FAni}^+$ was suppressed in the two-dimensional layer, where a small amplitude thermal fluctuation was identified by the potential energy calculation and dielectric responses. The two-dimensional $[\text{Ni}(\text{dmit})_2]^-$ anion layer was constructed from lateral sulfur–sulfur interatomic contacts along the long- and short-axes of the $[\text{Ni}(\text{dmit})_2]^-$ anion. The magnetic behavior showed ferromagnetic coupling with a Weiss temperature of +3.42 K, where the lateral interactions along the short-axis of the $[\text{Ni}(\text{dmit})_2]^-$ anion was important to achieve the ferromagnetic coupling. The introduction of molecular rotator structures into the ferromagnetic layer shows the potential to form a novel ferroelectric–ferromagnetic organic–inorganic hybrid material.

Acknowledgements

This work was supported in part by a Grant-in-Aid for Science Research from the Ministry of Education, Culture, Sports, Science, and Technology of Japan.

Notes and references

† Single crystals of salt 1 were obtained by the standard diffusion method in an H-shaped cell (CH_3CN ~50 mL). The green solution of $(n\text{-Bu}_4\text{N})[\text{Ni}(\text{dmit})_2]$ (30 mg) and a solution of $(m\text{-FAni}^+)(\text{BF}_4^-)$ (~60 mg)

and $\text{DCH}[18]\text{crown-6}$ (~100 mg) were slowly diffused during a period of two weeks.

Crystal data for 1: $\text{C}_{32}\text{H}_{43}\text{N}_9\text{O}_6\text{NFS}_{10}\text{Ni}$, $M_r = 935.99$, $T = 100$ K, triclinic, space group $P\bar{1}$ (no. 2), $Z = 2$, $a = 12.3990(6)$ Å, $b = 12.5367(5)$ Å, $c = 14.1216(6)$ Å, $\alpha = 95.4297(12)^\circ$, $\beta = 104.7569(14)^\circ$, $\gamma = 104.5606(13)^\circ$, $V = 2024.78(14)$ Å³. Of the 19625 reflections collected, 9072 are independent. On the basis of all these data and 461 refined parameters, $R(\text{int}) = 0.029$, $R_1(\text{observed data}) = 0.0363$ and $wR_2(\text{all data}) = 0.1310$ were obtained. $T = 300$ K, triclinic, space group $P\bar{1}$ (no. 2), $Z = 2$, $a = 12.4557(10)$ Å, $b = 12.7411(9)$ Å, $c = 14.2746(10)$ Å, $\alpha = 94.509(2)^\circ$, $\beta = 104.813(2)^\circ$, $\gamma = 105.509(2)^\circ$, $V = 2083.9(3)$ Å³. Of the 20345 reflections collected, 9365 are independent. On the basis of all these data and 461 refined parameters, $R(\text{int}) = 0.033$, $R_1(\text{observed data}) = 0.0437$ and $wR_2(\text{all data}) = 0.1568$ were obtained. Intensity data were collected on a Rigaku RAXIS-RAPID diffractometer using Mo-K α radiation. The structure was solved by direct methods and refined through the full-matrix least-squares method on F^2 using SHELXS-97.¹¹ CCDC number: 749640–749641.

Temperature-dependent dielectric constants were measured by the two-probe AC impedance method at frequencies from 1 to 1000 kHz (HP4194A). The electrical contacts were prepared using gold paste (Tokuriki 8560) to attach the 10- μm \varnothing gold wires to the single crystal. The temperature-dependent magnetic susceptibility and the magnetization-magnetic field dependence were measured using a Quantum Design MPMS-XL5 SQUID magnetometer using polycrystalline samples.

- J. S. Miller and A. J. Epstein, *Angew. Chem., Int. Ed. Engl.*, 1994, **33**, 385; O. Kahn, Y. Pei, M. Verdagner, J. P. Renard and J. Sletten, *J. Am. Chem. Soc.*, 1988, **110**, 782; H. Ohba, H. Okawa, N. Fukita and Y. Hashimoto, *J. Am. Chem. Soc.*, 1997, **119**, 1011.
- A. Rosa, G. Ricciardi and E. J. Baerends, *Inorg. Chem.*, 1998, **37**, 1368; R. Sarangi, G. S. DeBeer, D. Rudd, R. K. Szilagy, X. Ribas, C. Rovira, M. Almeida, K. O. Hodgson, B. Hedman and E. I. Solomon, *J. Am. Chem. Soc.*, 2007, **129**, 2316.
- A. T. Coomber, D. Beljonne, R. H. Friend, J. L. Brédas, A. Charlton, N. Robertson, A. E. Underhill, M. Kurmoo and P. Day, *Nature*, 1996, **380**, 144.
- T. Akutagawa and T. Nakamura, *Dalton Trans.*, 2008, 6335; T. Akutagawa, D. Sato, H. Koshinaka, M. Aonuma, S. Noro, S. Takeda and T. Nakamura, *Inorg. Chem.*, 2008, **47**, 5951.
- N. Takamatsu, T. Akutagawa, T. Hasegawa, T. Nakamura, T. Inabe, W. Fujita and K. Awaga, *Inorg. Chem.*, 2000, **39**, 870; T. Akutagawa, A. Hashimoto, S. Nishihara, T. Hasegawa and T. Nakamura, *J. Phys. Chem. B*, 2003, **107**, 66; S. Nishihara, T. Akutagawa, T. Hasegawa and T. Nakamura, *Chem. Commun.*, 2002, 408.
- T. Akutagawa, K. Shitagami, S. Nishihara, S. Takeda, T. Hasegawa, T. Nakamura, Y. Hosokoshi, K. Inoue, S. Ikeuchi, Y. Miyazaki and K. Saito, *J. Am. Chem. Soc.*, 2005, **127**, 4397; T. Akutagawa, H. Koshinaka, D. Sato, S. Takeda, S. Noro, H. Takahashi, R. Kumai, Y. Tokura and T. Nakamura, *Nat. Mater.*, 2009, **8**, 342.
- G. A. Jeffrey, *An Introduction to Hydrogen Bonding*, D. G. Truhlar Ed., Oxford University Press, New York, 1997.
- M. J. Frisch, G. W. Trucks, H. B. Schlegel, G. E. Scuseria, M. A. Robb, J. R. Cheeseman, J. A. Montgomery, Jr., T. Vreven, K. N. Kudin, J. C. Burant, J. M. Millam, S. S. Iyengar, J. Tomasi, V. Barone, B. Mennucci, M. Cossi, G. Scalmani, N. Rega, G. A. Petersson, H. Nakatsuji, M. Hada, M. Ehara, K. Toyota, R. Fukuda, J. Hasegawa, M. Ishida, T. Nakajima, Y. Honda, O. Kitao, H. Nakai, M. Klene, X. Li, J. E. Knox, H. P. Hratchian, J. B. Cross, V. Bakken, C. Adamo, J. Jaramillo, R. Gomperts, R. E. Stratmann, O. Yazyev, A. J. Austin, R. Cammi, C. Pomelli, J. Ochterski, P. Y. Ayala, K. Morokuma, G. A. Voth, P. Salvador, J. J. Dannenberg, V. G. Zakrzewski, S. Dapprich, A. D. Daniels, M. C. Strain, O. Farkas, D. K. Malick, A. D. Rabuck, K. Raghavachari, J. B. Foresman, J. V. Ortiz, Q. Cui, A. G. Baboul, S. Clifford, J. Cioslowski, B. B. Stefanov, G. Liu, A. Liashenko, P. Piskorz, I. Komaromi, R. L. Martin, D. J. Fox, T. Keith, M. A. Al-Laham, C. Y. Peng, A. Nanayakkara, M. Challacombe, P. M. W. Gill, B. G. Johnson, W. Chen, M. W. Wong, C. Gonzalez and J. A. Pople, *GAUSSIAN R03W (version 6.1)*, Gaussian, Inc., Wallingford, CT, 2004.
- H. Nagao, M. Nishio, Y. Shigeta, T. Soda, Y. Kitagawa, T. Onishi, Y. Yoshioka and K. Yamaguchi, *Coord. Chem. Rev.*, 2000, **198**, 265.
- P. Grosshans, P. Adkine, H. Sidorenkova, M. Nomura, M. Fourmigué and M. Gheffroy, *J. Phys. Chem. A*, 2008, **112**, 4067.
- G. M. Sheldrick, University of Göttingen, 1993/1997/2001.